RSC Advances

PAPER

View Article Online
View Journal | View Issue

Cite this: *RSC Adv.*, 2023, **13**, 25828

A study on rapid and stable catalytic reduction of 4-nitrophenol by 2-hydroxyethylamine stabilized Fe_3O_4@Pt and its kinetic factors†

Xia Xu, * Liming Yang, Yanjun Cui and Bing Hu

Received 5th August 2023
Accepted 24th August 2023

DOI: 10.1039/d3ra05298b

rsc.li/rsc-advances

The successful development of efficient and stable catalysts for 4-NP reduction reactions is beneficial to the environment and ecology. Fe_3O_4@Pt exhibits excellent catalytic performance for 4-NP reduction reaction due to the synergistic effect between Fe and Pt. But its structure and catalytic performance are extremely unstable. Here, we utilized the small-scale organic compound 2-hydroxyethylamine as surfactant to construct a stable composite nanomaterial. Then investigated the influence of monochromatic light (650 nm, 808 nm and 980 nm) and temperature on the kinetics of 4-NP reduction reaction by 2-hydroxyethylamine stabilized Fe_3O_4@Pt. The results indicate that both temperature and monochromatic light radiation can affect kinetic regulation. Increasing temperature can promote the catalytic rate, while monochromatic light radiation can induce agglomeration and inhibit the catalytic rate. This study opens up a new way for developing and regulating catalysts for heterogeneous catalysis reactions.

Introduction

4-Nitrophenol (4-NP) and nitroaromatic compounds are widely used as intermediates in pharmaceutical, pesticide and dye production.[1] Their poor biodegradability, high solubility, toxicity and stability in water have caused many ecological problems.[2–4] Therefore, most of the nitroaromatic compounds including 4-NP are listed as major pollutants by the U.S. Environmental Protection Agency.[5–7] However, the reduced product 4-aminophenol (4-AP) can serve as an intermediate in the synthesis of various analgesic and antipyretic drugs,[8] and other aniline derivatives, such as aniline, are important monomers for preparing functional polymers and can be widely used in materials science.[9–12] Catalytic reduction of 4-NP in aqueous to obtain 4-AP and similar derived aminophenols is not only environmentally friendly, but also easy to operate and detect, and has gradually developed into an important research field. Therefore, designing and synthesizing efficient and stable catalysts is crucial for this field.

So far, various noble metal nanocatalysts have been successfully applied to 4-NP reduction reactions, but their catalytic performance varies. The catalytic performance of precious metal nanocatalysts largely depends on the inherent physical and chemical properties of the catalyst's nanostructure and composition, such as Au,[13] Ag,[14] Pd,[15] Pt[16] and mutual bimetallic nanomaterials.[17–20] However, the agglomeration of precious nanocatalysts during catalytic reactions is inevitable.[21] In order to achieve more satisfactory stability, as well as improved catalytic activity and selectivity, multi-component composite nanocatalysts are the natural choices. Reduced graphene oxide,[22] polydopamine-wrapped reduced graphene oxide,[23] metal–organic framework,[24] carbon nanotubes,[25] as well as inorganic salts $CaCO_3$ (ref. 26) and γ-Al_2O_3,[27] can all be used as support materials to construct composite nanomaterials with precious metals. In addition, support materials can also change the intrinsic electronic properties of metal nanoparticles or generate catalytic active site at the metal support interface through metal–support interaction, providing a key contribution to the overall catalytic activity.[28–32]

Although organic surfactants with large size and polymer hydrogels can be used to improve the stability of precious nanocatalysts, the surfactants or polymer hydrogels usually passivate the active surface, resulting in loss of catalytic activity or too long induction time.[33–35] In our research group's published articles, large-sized sodium bicarbonate crystals can be used to improve the stability of Fe_2O_3@Pt, the residual polymer SiO_2 usually passivates the active surface, leading to a loss of catalytic activity or long induction time.[36]

In addition, as suggested by Arrhenius equation, the rate of some catalytic reactions can be further increased by increasing the local temperature of the active site on the catalyst surface.[37] Another method for regulating reaction kinetics is photoradiation, but most studies are based on the photothermal conversion of photothermal reagents or the localized surface plasmon resonance (LSPR) coupling effect to change the temperature of the solution to explore its impact on catalytic reduction performance.[38–42] However, there are few reports on

College of Science, Gansu Agricultural University, No.1, Yingmen Village, Lanzhou 730070, P. R. China. E-mail: xuxia@gsau.edu.cn

† Electronic supplementary information (ESI) available. See DOI: https://doi.org/10.1039/d3ra05298b

the effect of monochromatic light radiation on catalytic rate without causing temperature changes in the solution.

Herein, Fe_3O_4 has been chosen as a carrier for loading Pt atomic clusters due to its ability to be adsorbed by magnets and its ease of separation and recovery. Organic surfactant 2-hydroxyethylamine with small size is adsorbed on the surface of Fe_3O_4@Pt composite nanomaterials to prevent the separation and aggregation of Pt and Fe_3O_4, and excessive 2-hydroxyethylamine can form a supporting membrane, thereby stabilizing its structural characteristics without affecting its catalytic performance. In addition, the influence of monochromatic light (650 nm, 808 nm and 980 nm) and temperature on the catalytic reduction of 4-nitrophenol were investigated *via* 2-hydroxyethylamine stabilized Fe_3O_4@Pt.

Experimental section

Materials

Chloroplatinic acid hexahydrate ($H_2PtCl_6 \cdot 6H_2O$) and 4-nitrophenol (4-NP) were obtained from Aladdin reagent (Shanghai) Co., Ltd. Ethanol was obtained from Beijing Chemical Reagent. $FeSO_4$ was obtained from Sinopharm Chemical Reagent Co., Ltd. $NaBH_4$ was obtained from Jinan Yuxin Chemical Co., Ltd. 2-Hydroxyethylamine purchased from Yantai Shuangshuang Chemical Co., Ltd. All reagents used in this study are analytically pure and have not been purified in any way except for special labels. All experiments used deionized water.

Synthesis of Fe_3O_4@Pt

First, distilled water (5 mL) and $FeSO_4$ (4 mg) were added into a 50 mL beaker for ultrasonic dispersion. Then add ethanol (5 mL) and H_2PtCl_6 aqueous solution (0.2 mL, 1 g/100 mL). After fully stirring, $NaBH_4$ powder (5 mg) was added into the mixed system. After stirring for 10 minutes, centrifuge and separate. Discard the supernatant, wash the sediment with distilled water, and then disperse the sediment in 2 mL distilled water for standby.

Synthesis of 2-hydroxyethylamine stabilized Fe_3O_4@Pt

The preparation method of 2-hydroxyethylamine stabilized Fe_3O_4@Pt is the same as that of Fe_3O_4@Pt, but the difference is that different amounts of 2-hydroxyethylamine (0, 0.1, 0.2, 0.3, 0.4 and 0.5 mL) need to be added at the same time as 5 mg $NaBH_4$.

The catalytic reduction performance test for 4-NP

The catalytic reduction performance test was conducted using a 4 mL quartz cuvette as the reaction vessel at room temperature. The specific operating steps are as follows: H_2O (3 mL), 4-NP (20 μL, 0.01 mol L^{-1}), Fe_3O_4@Pt or 2-hydroxyethylamine stabilized Fe_3O_4@Pt (20 μL, 0.001931 mol L^{-1}, taking from 2 mL stock solution) were successively added into a 4 mL quartz colorimetric dish. After the solution was completely dispersed evenly, fresh $NaBH_4$ (100 μL, 0.2 mol L^{-1}) aqueous solution is dropped into the above solution. The molar ratio of $NaBH_4$/4-NP is 100, so the amount of $NaBH_4$ is excess compared to 4-NP. The absorbance performance during reaction was monitored by UV-vis spectra (in the range of 250–500 nm) or 722N spectrophotometer (record the absorbance value at $\lambda = 400$ nm).

The catalytic reduction performance test under different temperatures and light radiation is similar to the above method, except that before starting the test, the aqueous solution containing 4-NP and catalyst is heated to constant temperature in a constant temperature water bath or continuously irradiated for 1 minute under a specific wavelength and power of laser.

Characterization

The powder X-ray diffraction (XRD) pattern was measured on a Panaco X′ Pert PRO X-ray diffractometer with Cu Ka radiation ($l = 0.15406$ nm, the operation voltage: 45 kV, the operation current: 40 mA, scanning speed: 1° min^{-1}, test range: $10° \leq 2\theta \leq 70°$). The transmission electron microscope (TEM) images were obtained on a FEI Talos F200S transmission electron microscope (the operation voltage: 200 kV). The Fine spectra of Fe and Pt were determined by Thermo ESCALAB 250XI X-ray photoelectron spectroscopy (XPS). The magnetometer hysteresis loops was measured on LakeShore 7404. The UV-vis absorption spectra were measured on Shimadzu UV-1780 UV-vis-NIR spectrophotometer. The absorbance at $\lambda = 400$ nm was monitored by a 722N visible spectrophotometer.

Results and discussion

Synthesis and characterization of 2-hydroxyethylamine stabilized Fe_3O_4@Pt

Fig. 1 shows the XRD results of Fe_3O_4@Pt and 2-hydroxyethylamine stabilized Fe_3O_4@Pt, the diffraction peak at about 40° is attributed to Pt nanoparticles, and the other diffraction peaks are consistent with the cubic phase of Fe_3O_4 (JCPDS: 75-0449). A series of weak diffraction peaks were observed in 35.76, 57.51 and 63.17, corresponding to (311), (511) and (440) crystal planes, respectively. When 2-hydroxyethylamine is added, 2-hydroxyethylamine adsorbs on the surface of the composite nanomaterial, so the diffraction peak of Fe_3O_4 weakens significantly. What's more, 2-hydroxyethylamine stabilized Fe_3O_4@Pt has the ability to be adsorbed by magnets and is easy to separate and recover. Its saturation magnetization, residual magnetic field strength and coercive force were 27.9 emu g^{-1}, 5.9 emu g^{-1} and 138.7 G, respectively (Fig. S1†). The TEM images of Fe_3O_4@Pt (Fig. 2a and b) show that Pt clusters of approximately 2 nm uniformly dot the surface of Fe_3O_4, and the overall uniformity and dispersion are particularly good. But this structure is extremely unstable, and Pt and Fe_3O_4 will quickly separate and aggregate when stored in aqueous solution for 3 hours (Fig. 2c and d). Fig. 2e and f show the TEM images of 2-hydroxyethylamine stabilized Fe_3O_4@Pt. 2-Hydroxyethylamine can adsorb on the surface of composite nanomaterials to form a protective layer, preventing the separation and aggregation of Pt and Fe_3O_4, and the excess can spontaneously form a supporting membrane, thereby improving the stability of composite nanocatalysts. As shown in Fig. S2,† the addition of

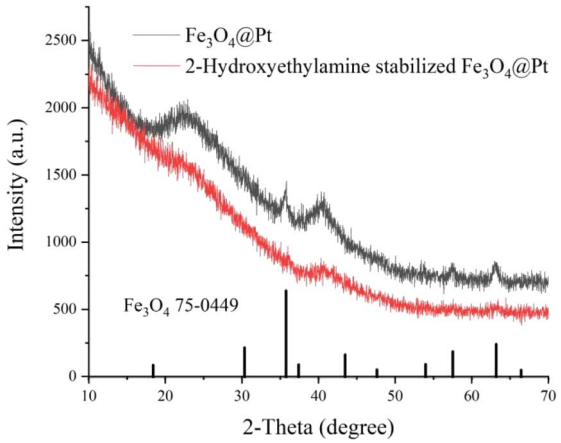

Fig. 1 X-ray powder diffraction (XRD) patterns of Fe_3O_4@Pt and 2-hydroxyethylamine stabilized Fe_3O_4@Pt.

2-hydroxyethylamine has no effect on the XPS fine spectra of Fe 2p and Pt 4f. The high-resolution XPS spectra of Fe 2p (Fig. 3a) indicated that 2-hydroxyethylamine stabilized Fe_3O_4@Pt were primarily composed of Fe^{2+} corresponded to the peaks at 710.2 eV and 723.3 eV, and the peaks at 711.7 and 725.1 eV were assigned to Fe^{3+}. The two valence states of Fe element are consistent with XRD results, which once again confirms that the crystal phase of the prepared sample is Fe_3O_4. The peaks at 71.1 and 74.4 eV were originated from the presence of metallic Pt (Fig. 3b).

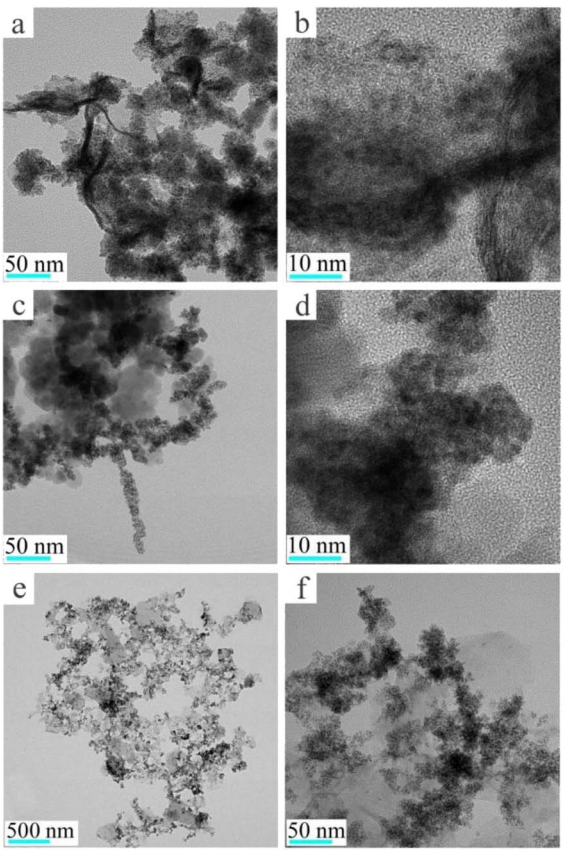

Fig. 2 Transmission electron microscopy (TEM) images of (a and b) freshly prepared Fe_3O_4@Pt, (c and d) Fe_3O_4@Pt after 3 hours of storage, (e and f) 2-hydroxyethylamine stabilized Fe_3O_4@Pt.

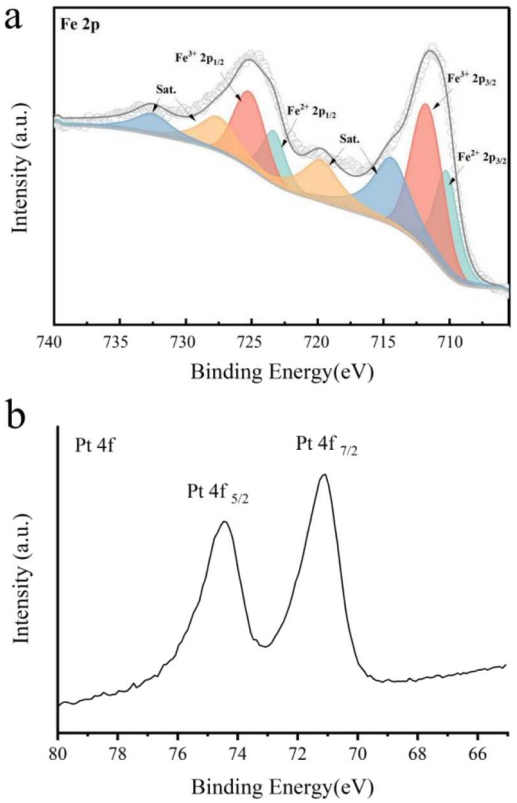

Fig. 3 XPS high-resolution spectra of (a) Fe 2p and (b) Pt 4f of 2-hydroxyethylamine stabilized Fe_3O_4@Pt.

Catalytic reduction performance of 2-hydroxyethylamine stabilized Fe_3O_4@Pt for 4-NP

The catalytic reduction of 4-NP to 4-AP in aqueous phase has become an important research field. On the contrary, because of its simplicity and repeatability, the catalytic reduction of 4-NP with $NaBH_4$ under aqueous phase has become a benchmark model reaction to quantify the catalytic activity of 2-hydroxyethylamine stabilized Fe_3O_4@Pt. As shown in Fig. S3,† the intensity of absorption peak at 400 nm belongs to the 4-NP, 20 μL, 1.9 mM 2-hydroxyethylamine stabilized Fe_3O_4@Pt can trigger the decrease of the absorption peak at 400 nm, and the formation of a new peak belongs to 4-AP at 300 nm. Therefore, the absorbance value at 400 nm could represent the concentration of 4-NP, and the reduction process can be easily monitored using a 722N spectrophotometer. Since the amount of $NaBH_4$ is excess compared to 4-NP, the reaction kinetics follows the pseudofirst-order law, the apparent kinetic rate constant k_{app} can be described as eqn (1):

$$-\ln\frac{A_t}{A_0} = -\ln\frac{C_t}{C_0} = k_{app}t \quad (1)$$

where C_0 and A_0 stand for the initial concentration and absorbance of 4-NP, while C_t and A_t correspond to time t.

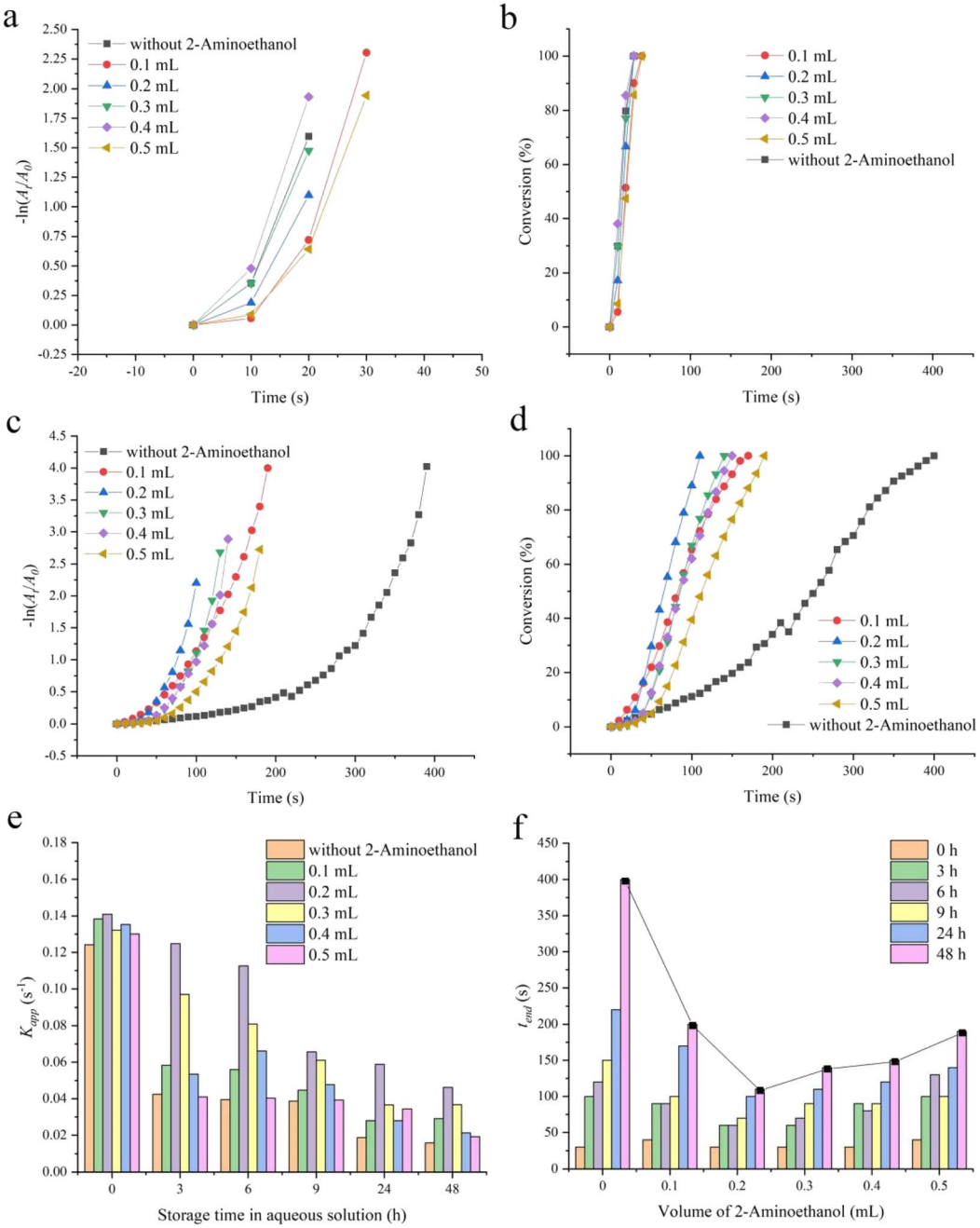

Fig. 4 Plots of $-\ln(A_t/A_0)$ and conversion *versus* the reaction time t for 4-NP catalyzed by 2-hydroxyethylamine stabilized Fe_3O_4@Pt under different conditions: (a and b) freshly prepared, (c and d) after 48 hours of storage. (e and f) Plots of reaction rate k_{app} and reaction end time t_{end} *versus* the reaction time t under different amounts of 2-hydroxyethylamine and storage time. All reactions take place at room temperature, the catalyst concentration is 0.013 mM, and the molar ratio of $NaBH_4$/4-NP is 100.

As a confirmatory experiment, the catalytic reduction performance of a series of 2-hydroxyethylamine (0, 0.1, 0.2, 0.3, 0.4 and 0.5 mL) stabilized Fe_3O_4@Pt for 4-NP were characterized. As can be seen in Fig. 4a, the catalytic effect of 2-hydroxyethylamine stabilized Fe_3O_4@Pt under different amounts of 2-hydroxyethylamine are all excellent, a small quantity of catalysts (20 μL, 1.9 mM) with different specifications can trigger the 100% conversion of 4-NP to 4-AP within merely 40 s (Fig. 4b). When the catalyst is stored in aqueous solution for 48 h, the catalytic effect of 2-hydroxyethylamine stabilized Fe_3O_4@Pt for 4-NP is much better than that without 2-hydroxyethylamine, and the conversion efficiency of 4-NP by 2-hydroxyethylamine stabilized Fe_3O_4@Pt was up to 100% in 200 s, which was significantly higher than that without 2-hydroxyethylamine (Fig. 4c and d). The catalytic reduction process of 4-NP with different specifications of catalysts under different storage times were shown in Fig. S4–S6.† As described in eqn (1), there is a linear relationship between $-\ln(A_t/A_0)$ and t. The apparent

Table 1 Comparison of the kinetic parameter of 2-hydroxyethylamine stabilized Fe_3O_4@Pt for 4-NP with that of previous work. In this work, the catalyst concentration is measured by Pt concentration

Catalyst	Reaction time	4-NP concentration (mM)	Catalyst concentration	Rate constant (10^{-3} s^{-1})	TOF/h^{-1}	Ref.
Pd/RGO/Fe_3O_4	60 s	2.5	5 mg	51	—	43
Pd-GA/RGO	5 min	5	1–20 mg	7	—	44
Cu/Pd@graphitic carbon	—	0.05	0.083 mM	80	108	45
AgNPs/SiNSs	40 s	0.12	0.051 mM	80	200	46
PtAu-PDA/RGO	3 min	0.1	0.01 mM	9.58	200	47
Sodium sesquicarbonate-supporting Fe_2O_3@Pt	4 min	0.067	0.013 mM	13.98	78	36
2-Hydroxyethylamine stabilized Fe_3O_4@Pt	30 s	0.067	0.013 mM	90.93	621	This work

kinetic rate constant k_{app} of different specifications of catalysts under different storage times was shown in Fig. 4e. Although k_{app} decreases with increasing storage time, Fe_3O_4@Pt protected with 0.2 mL 2-hydroxyethylamine has always been the optimal catalytic rate (0.1409 s^{-1} for newly prepared and 0.04615 s^{-1} for storage after 48 h) and the shortest reaction time t_{end} (30 s for newly prepared and 110 s for storage after 48 h) (Fig. 4f). The author characterized the TEM image of 2-hydroxyethylamine stabilized Fe_3O_4@Pt under different amounts of 2-hydroxyethylamine (0.2 mL and 0.5 mL). As shown in Fig. S7,† the amount of 2-hydroxyethylamine does not change the particle size and textural properties, but excessive 2-hydroxyethylamine will completely adsorb on the surface of Fe_3O_4@Pt, even encapsulating Fe_3O_4@Pt, thus passivating the active surface and reducing its catalytic activity. Therefore, the experiment confirmed that 2-hydroxyethylamine indeed has a protective effect on the Fe_3O_4@Pt structure, and 0.2 mL is the optimal amount. For comparing our catalytic reduction effect

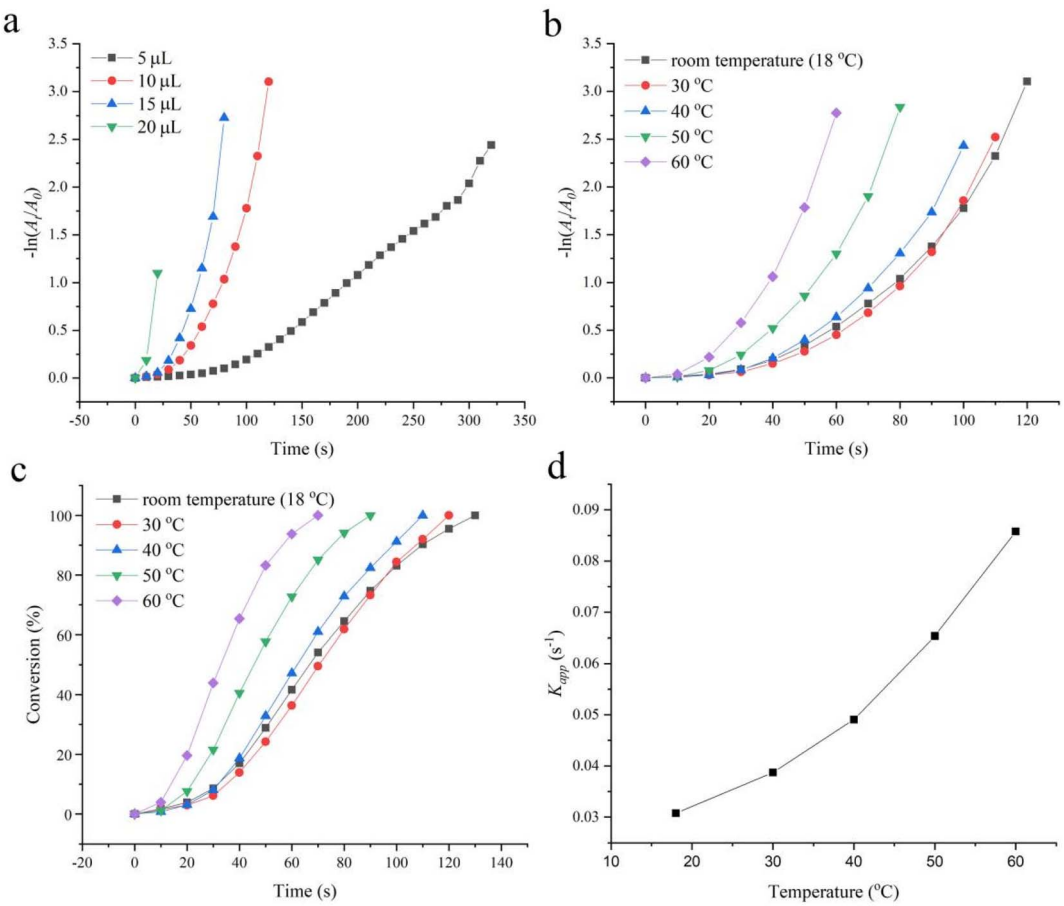

Fig. 5 Plots of $-\ln(A_t/A_0)$ *versus* the reaction time t for 4-NP under (a) different dosages of catalysts, (b) different reaction temperatures. (c) Time dependent conversion of 4-NP at different temperatures and (d) the trend of reaction rate k_{app} changing with temperature.

for 4-NP with those reported catalysts, the turnover frequency TOF, defined as moles of reactant reduced through per mole of catalyst per second, was calculated to be 621 h^{-1} for newly prepared, and 166 h^{-1} for storage after 48 h. The TOF value is much higher than that of noble metal catalysts (Table 1), indicating that 2-hydroxyethylamine stabilized Fe_3O_4@Pt has excellent catalytic reduction activity for 4-NP. Finally, the reusability of 2-hydroxyethylamine stabilized Fe_3O_4@Pt was characterized. As shown in Fig. S8,† the catalytic performance remains good after 5 cycles, once again verifying the excellent catalytic stability of 2-hydroxyethylamine stabilized Fe_3O_4@Pt.

The effect of temperature on the catalytic reduction performance of 2-hydroxyethylamine stabilized Fe_3O_4@Pt for 4-NP

As we previously described, the catalytic rate of 20 μL, 0.013 mM 2-hydroxyethylamine stabilized Fe_3O_4@Pt for 4-NP was too high (the apparent kinetic rate constant $K_{app} = 0.1409\ s^{-1}$) to analyze the effect of temperature on its catalytic performance. So the amount of catalyst (5, 10, 15 and 20 μL) was carefully investigated. As presented in Fig. 5a, 10 μL, 0.013 mM 2-hydroxyethylamine stabilized Fe_3O_4@Pt has a relatively moderate catalytic rate ($K_{app} = 0.03075\ s^{-1}$) and is applied to explore the effect of temperature for 4-NP. As shown in Fig. 5b–d, the conversion efficiency and reaction rates K_{app} increase with the increase of reaction temperature. When the reaction reaches 60 s, the conversion of the 60 °C system has reached 100%, while that of the room temperature system is only 54.14%. The temperature increased from 18 °C to 60 °C, k_{app} increased from 0.03075 to 0.08579 s^{-1}, an increase of 2.8 times. The TOF also increased from 305.87 to 582.82 h^{-1}, an increase of 1.9 times. The results as suggested by Arrhenius equation,[37] the catalytic rate for 4-NP can be further increased by increasing the local temperature of the active site on the catalyst surface. Meanwhile, it has been proven that 2-hydroxyethylamine stabilized Fe_3O_4@Pt has good thermal stability.

The effect of light on the catalytic reduction performance of 2-hydroxyethylamine stabilized Fe_3O_4@Pt for 4-NP

Another method of adjusting reaction kinetics is to change the temperature of the catalyst surface through photothermal transformation. However, most photothermal research is based on converting light energy into thermal energy through photothermal materials to increase the temperature of the entire solution and explore changes in catalytic performance.[38–42] This manuscript explores the effect of light radiation on catalytic efficiency without increasing the entire solution temperature. As shown in Fig. S9,† 2-hydroxyethylamine stabilized Fe_3O_4@Pt has absorption throughout the entire UV visible and near-infrared regions. Therefore, three types of monochromatic light with

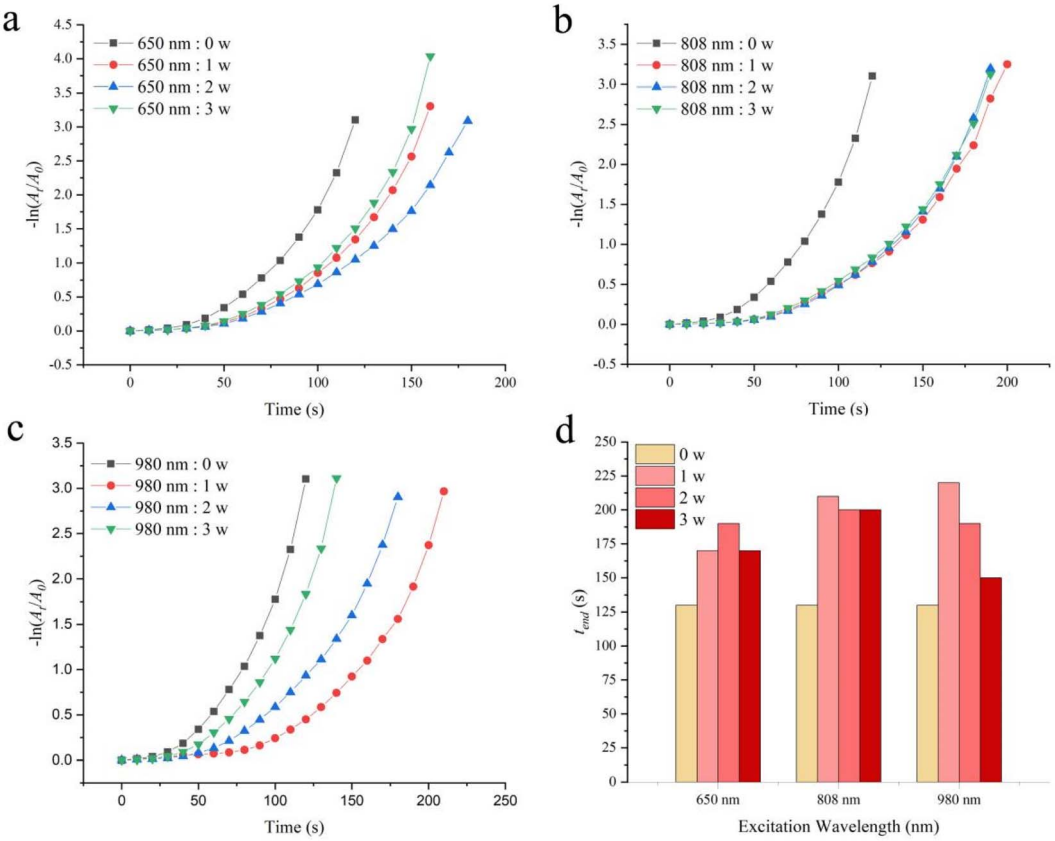

Fig. 6 Plots of $-\ln(A_t/A_0)$ *versus* the reaction time t for 4-NP under different wavelengths and power light radiation: (a) 650 nm, (b) 808 nm, (c) 980 nm. (d) The relationship between reaction end time t_{end} and radiation wavelength and radiation power.

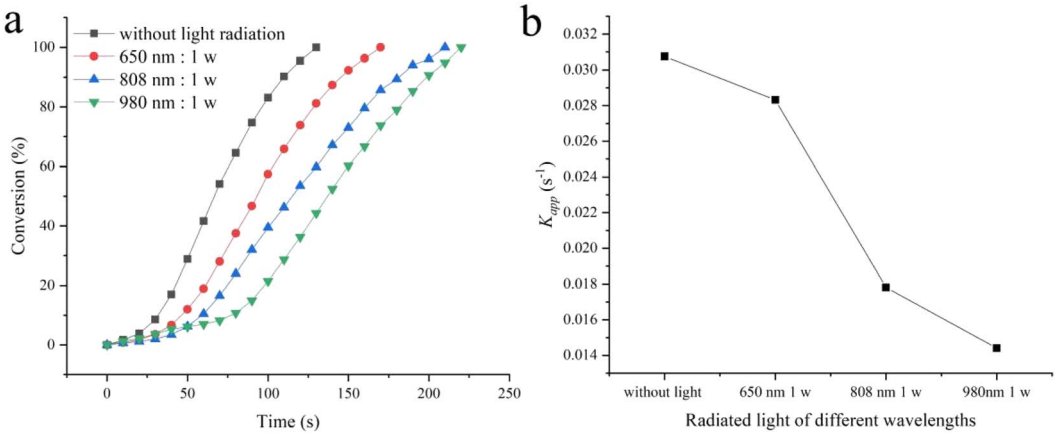

Fig. 7 (a) The conversion *versus* the reaction time *t* for 4-NP under different wavelengths of radiation light at 1 w, (b) the trend of reaction rate k_{app} changing with radiation wavelength at 1 w.

good penetrability (650 nm, 808 nm and 980 nm) were selected to explore the impact of light radiation on catalytic performance. Fig. S10† shows the temperature changes of aqueous solutions caused by light radiation at different radiation wavelengths and powers. 650 nm monochromatic light with power of 1 w, 2 w, and 3 w continuously radiated for 60 s, causing little thermal effect and no change in solution temperature. The 808 nm radiation caused minimal thermal effect, leading to an increase in solution temperature of 1 °C for 1 w and 2 °C for 2–3 w. However, 980 nm radiation causes significant thermal effects, 3 °C for 1 w, 7 °C for 2 w and 10 °C for 3 w. The effect of light on the catalytic reduction performance of 2-hydroxyethylamine stabilized Fe_3O_4@Pt for 4-NP is shown in Fig. 6. Under different wavelengths and power radiation, it causes a decrease in catalytic rate and an extension of catalytic reaction end time t_{end}. For 650 nm and 808 nm monochromatic light, the thermal effect caused by power changes is not significant, so the catalytic rate does not change significantly at different powers (Fig. 6a and b). However, for 980 nm monochromatic light, the thermal effect caused by the increase in power is significant, so the catalytic rate gradually increases (Fig. 6c). Fig. 7 compares the effect of different wavelengths of radiation light at 1 w on the catalytic reduction for 4-NP. The comparison results clearly indicate that as the wavelength increases, the conversion rate and catalytic rate both significantly decrease (the k_{app} without light radiation, at 650 nm, 808 nm, and 980 nm radiation are 0.03075, 0.02832, 0.01781, and 0.01441 s^{-1}, respectively). Therefore, it can be concluded that monochromatic light radiation has an inhibitory effect on 2-hydroxyethylamine stabilized Fe_3O_4@Pt catalytic reduction of 4-NP, and the longer the wavelength, the more obvious the inhibitory effect. The inhibition effect caused by monochromatic radiation may be attributed to the aggregation of Pt clusters driven by photogenerated electrons and their transfer to surface Pt atoms.[48]

Conclusions

In summary, 2-hydroxyethylamine stabilized Fe_3O_4@Pt composite nanocatalyst is developed *via* a one-pot route. The composite nanocatalyst exhibits a stable and enhanced catalytic performance for 4-NP reduction reaction. The value of the reaction rate k_{app} and TOF are also higher than many other reported catalysts. Moreover, the dynamic adjustment experiment shows that increasing temperature can promote the catalytic rate, while monochromatic light radiation (650 nm, 808 nm and 980 nm) inhibits the catalytic rate. In conclusion, we believe that 2-hydroxyethylamine stabilized Fe_3O_4@Pt composite nanocatalyst will have wide application attraction in 4-NP reduction reaction.

Conflicts of interest

There are no conflicts to declare.

Acknowledgements

The authors are grateful for the financial aid from the National Natural Science Foundation of China (Grant No. 21961001) and the institution of higher education of Gansu Province Foundation for Young doctor (2022QB-079).

Notes and references

1 Y. Wang, Y. Xie, H. Sun, J. Xiao, H. Cao and S. Wang, *Catal. Sci. Technol.*, 2016, **6**, 2918.
2 W. J. Liu, K. Tian, H. Jiang and H. Q. Yu, *Green Chem.*, 2014, **16**, 4198.
3 Y. Liu, Y. Fan, Y. Yuan, Y. Chen, F. Cheng and S. C. Jiang, *J. Mater. Chem.*, 2012, **22**, 21173.
4 F. Wang, S. Y. Song, K. Li, J. Q. Li, J. Pan, S. Yao, X. Ge, J. Feng, X. Wang and H. J. Zhang, *Adv. Mater.*, 2016, **28**, 10679.
5 Y. Q. Jiang, J. J. Zhang and R. Balasubramanian, *J. Environ. Chem. Eng.*, 2022, **10**, 107215.
6 Y. X. He, N. Cheshomi, S. M. Lawson, A. K. Itta, F. Reazei, S. Kapila and A. A. Rownaghi, *Chem. Eng. J.*, 2021, **410**, 128326.
7 K. P. Mishra and P. R. Gogate, *Ultrason. Sonochem.*, 2011, **18**, 739.

8 F. Coccia, L. Tonucci, D. Bosco, M. Bressan and N. d'Alessandro, *Green Chem.*, 2012, **14**, 1073.
9 C. Li, L. Zhu, L. Song, G. Zhu, Q. Zhang, Y. Zhao, Q. Gong, C. Sun, Y. Liu, K. Sasakid and J. Xie, *J. Mater. Chem. A*, 2023, **11**, 7756.
10 W. Li, F. Wang, Y. Shi and L. Yu, *Chin. Chem. Lett.*, 2023, **34**, 107505.
11 H. Wan, C. Qin and A. Lu, *J. Mater. Chem. A*, 2022, **10**, 17279.
12 Z. Zeng, Y. Chen, X. Zhu and L. Yu, *Chin. Chem. Lett.*, 2023, **34**, 107728.
13 P. Zhao, X. Feng, D. Huang, G. Yang and D. Astruc, *Coord. Chem. Rev.*, 2015, **287**, 114.
14 P. Zhang, C. Shao, Z. Zhang, M. Zhang, J. Mu, Z. Guo and Y. Liu, *Nanoscale*, 2011, **3**, 3357.
15 Q. Wang, W. Jia, B. Liu, A. Dong, X. Gong, C. Li, P. Jing, Y. Li, G. Xua and J. Zhang, *J. Mater. Chem. A*, 2013, **1**, 12732.
16 S. K. Ghosh, M. Mandal, S. Kundu, S. Nath and T. Pal, *Appl. Catal., A*, 2004, **268**, 61.
17 Z. Dong, X. Le, C. Dong, W. Zhang, X. Li and J. Ma, *Appl. Catal., B*, 2015, **162**, 372.
18 M. Nasrollahzadeh, S. M. Sajadi, A. Rostami-Vartooni and M. Bagherzadeh, *J. Colloid Interface Sci.*, 2015, **448**, 106.
19 X. F. Tan, J. Qin, Y. Li, Y. T. Zeng, G. X. Zheng, F. Feng and H. Li, *J. Hazard. Mater.*, 2020, **397**, 122786.
20 J. Qin, X. F. Tan, F. Feng and H. Li, *Appl. Surf. Sci.*, 2021, **561**, 150024.
21 M. Nasrollahzadeh and A. Banaei, *Tetrahedron Lett.*, 2015, **56**, 500.
22 A. T. Ezhil Vilian, S. R. Choe, K. Giribabu, S. C. Jang, C. Roh, Y. S. Huh and Y. K. Han, *J. Hazard. Mater.*, 2017, **333**, 54.
23 W. Ye, J. Yu, Y. Zhou, D. Gao, D. Wang, C. Wang and D. Xue, *Appl. Catal., B*, 2016, **181**, 371.
24 Z. Dong, X. Le, Y. Liu, C. Dong and J. Ma, *J. Mater. Chem. A*, 2014, **2**, 18775.
25 C. H. Liu, J. Liu, Y. Y. Zhou, X. L. Cai, Y. Lu, X. Gao and S. D. Wang, *Carbon*, 2015, **94**, 295.
26 Q. Ding, Z. Kang, L. Cao, M. Lin, H. Lin and D. P. Yang, *Appl. Surf. Sci.*, 2020, **510**, 145526.
27 F. Saira, N. Firdous, R. Qureshi and A. Ihsan, *Turk. J. Chem.*, 2020, **44**, 448.
28 Q. Fu, H. Saltsburg and M. Flytzani-Stephanopoulos, *Science*, 2003, **301**, 935.
29 M. Valden, X. Lai and D. W. Goodman, *Science*, 1998, **281**, 1647.
30 M. Cargnello, V. V. T. Doan-Nguyen, T. R. Gordon, R. E. Diaz, E. A. Stach, R. J. Gorte, P. Fornasiero and C. B. Murray, *Science*, 2013, **341**, 771.
31 X. Y. Liu, M. H. Liu, Y. C. Luo, C. Y. Mou, S. D. Lin, H. K. Cheng, J. M. Chen, J. F. Lee and T. S. Lin, *J. Am. Chem. Soc.*, 2012, **134**, 10251.
32 J. L. Shi, *Chem. Rev.*, 2013, **113**, 2139.
33 S. Saha, A. Pal, S. Kundu, S. Basu and T. Pal, *Langmuir*, 2010, **26**, 2885.
34 W. C. Elias, R. Eising, T. R. Silva, B. L. Albuquerque, E. Martendal, L. Meier and J. B. Domingos, *J. Phys. Chem. C*, 2014, **118**, 12962.
35 S. M. Ansar and C. L. Kitchens, *ACS Catal.*, 2016, **6**, 5553.
36 X. Xu, M. Li, L. Yang and B. Hu, *RSC Adv.*, 2023, **13**, 13556.
37 K. J. Laidler, *J. Chem. Educ.*, 1984, **61**, 494.
38 K. Wang, X. Zhu, Y. Yang, D. Ye, R. Chen and Q. Liao, *J. Environ. Chem. Eng.*, 2022, **10**, 108253.
39 M. Kang and Y. Kim, *J. Ind. Eng. Chem.*, 2020, **86**, 61.
40 J. H. Kim, B. W. Lavin, B. W. Boote and J. A. Pham, *J. Nanopart. Res.*, 2012, **14**, 995.
41 Y. Gu, Y. Jiao, X. Zhou, A. Wu, B. Buhe and H. Fu, *Nano Res.*, 2018, **11**, 126.
42 Z. Wang, W. Wang, M. Wamsley, D. Zhang and H. Wang, *ACS Appl. Mater. Interfaces*, 2022, **14**, 17560.
43 M. Atarod, M. Nasrollahzadeh and S. M. Sajadi, *J. Colloid Interface Sci.*, 2016, **465**, 249.
44 A. Vilian, S. R. Choe, K. Giribabu, S. Jang, C. Roh, Y. S. Huh and Y. Han, *J. Hazard. Mater.*, 2017, **333**, 54.
45 M. Morales, M. Rocha, C. Freire, E. Asedegbega-Nieto, E. Gallegos-Suarez, I. Rodríguez-Ramos and A. Guerrero-Ruiz, *Carbon*, 2017, **111**, 150.
46 Z. Yan, L. Fu, X. Zuo and H. Yang, *Appl. Catal., B*, 2018, **226**, 23.
47 W. Ye, J. Yu, Y. Zhou, D. Gao, D. Wang, C. Wang and D. Xue, *Appl. Catal., B*, 2016, **181**, 371.
48 N. Denisov, S. Qin, J. Will, B. N. Vasiljevic, N. V. Skorodumova, I. A. Pašti, B. B. Sarma, B. Osuagwu, T. Yokosawa, J. Voss, J. Wirth, E. Spiecker and P. Schmuki, *Adv. Mater.*, 2023, **35**, 2206569.